Analytica Chimica Acta 909 (2016) 101–108

Contents lists available at ScienceDirect

Analytica Chimica Acta

journal homepage: www.elsevier.com/locate/aca

Colorimetric detection of hepatitis B virus (HBV) DNA based on DNA-templated copper nanoclusters

Xiaoxia Mao [a, b], Siyu Liu [a], Chao Yang [a], Fengzhen Liu [c], Keming Wang [c, **], Guifang Chen [a, *]

[a] Laboratory of Biosensing Technology, School of Life Sciences, Shanghai University, Shanghai 200444, China
[b] Department of Life Science, Anqing Normal University, Anqing, Anhui 246011, China
[c] Department of Oncology, The Second Affiliated Hospital of Nanjing Medical University, Nanjing 210011, China

HIGHLIGHTS

- A colorimetry was designed for detection of DNA based on copper nanoclusters.
- This method is ability to be monitored with the naked eye.
- This method was successfully used for the analysis of Hepatitis B virus DNA.
- The colorimetric detection exhibited excellent sensitivity.

GRAPHICAL ABSTRACT

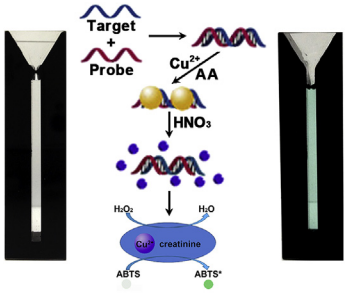

ARTICLE INFO

Article history:
Received 15 October 2015
Received in revised form
31 December 2015
Accepted 3 January 2016
Available online 11 January 2016

Keywords:
DNA
Hepatitis B virus
Colorimetry
Copper nanoclusters
Catalysis
Biosensor

ABSTRACT

DNA detection plays an important role in early diagnosis of genetic disease. The conventional detection methods of DNA are based on expensive equipment, which do not meet the demands of developing countries. Thus, we developed a colorimetric method, which could be observed with naked eye and used copper nanoclusters for cost-effective. Moreover, the target of this method is the DNA in Hepatitis B virus that is one of the most popular chronic viral infections in developing countries over the past years. Our method was sensitive and the limit of detection was 12×10^9 molecules. Three-base-pair mismatches target DNA was detected easily. These results revealed the favorable sensitivity and selectivity of this approach. Most importantly, our method may have potential applications in correct diagnosis of genetic disease and monitoring of gene therapy in the poverty-stricken areas.

© 2016 Elsevier B.V. All rights reserved.

1. Introduction

The detection and identification of specific nucleotide sequences (either DNA or RNA) is an enabling technology for a number of fields, including environmental monitoring, the recognition of genetic mutations, forensic analysis, and disease diagnosis [1]. Although nucleotide acid detection plays an important role in

* Corresponding author.
** Corresponding author.
E-mail addresses: wkmys@sohu.com (K. Wang), gfchen@shu.edu.cn (G. Chen).

http://dx.doi.org/10.1016/j.aca.2016.01.009
0003-2670/© 2016 Elsevier B.V. All rights reserved.

the diagnosis of genetic diseases and useful for early-stage treatment, conventional analysis methods still have many shortages. For example, southern blot relies on fluorescence and radioactive probes, which are often criticized for expensiveness and toxicity [2,3]. Conventional methods for the analysis of specific gene sequences are carried out using polymerase chain reaction (PCR). Although it is simple and effective for the detection of PCR products, many PCR related methods establish on high-precision instruments to perform specific conditions for consistent amplification. Unfortunately, such equipment is bulky, expensive and complex to operate. Although these analysis methods are commonly used in the world, they are often poorly suited for the developing world, where availability of clinical and laboratory facilities may be limited. The development of novel DNA detection method to meet the requirements of developing countries should therefore be focused on: (1) expensive instrument should be avoided and visual detection should be preferred. (2) Select appropriate cost-effective materials for application in low resource areas. In recent decades, various methods for detection of DNA have been emerged [4–6]. Among these methods, colorimetric method is readily visible to the naked eye [7]. Colorimetric method is thus extremely attractive in low resource areas. Thereby, in order to meet demands of developing countries, we designed a colorimetric method.

Nanomaterials, consisting of several to some tens of atoms, currently attract considerable attention for exhibiting unusual magnetic, electric, and catalytic characteristics [8]. Particularly, the noble-metal nanoclusters (NCs) have been found to exhibit molecular-like properties such as strong fluorescence [9]. These properties made metal NCs excellent candidates for sensing and bio-imaging of DNA [10]. The rational utilization of NCs (Au, Ag and Pt) to construct nucleic acid detection methods has been attracted significant interests [11–14]. Mokhir et al. reported that double-stranded DNA (dsDNA) can act as an efficient template for the formation of CuNCs at a low concentration of copper sulfate [15]. What's more, compared to other nanomaterials, CuNCs show more significant advantages because of low cost [16]. CuNCs based detection techniques are likely to meet the demand of developing countries.

Hepatitis B virus (HBV), a circular double-stranded oligonucleotides virus, causes chronic infections of the liver in humans [17]. HBV affects the daily lives of millions of people all around the world, especially in the developing countries [18]. According to World Health Organization, almost 240 million people are infected by HBV worldwide, and 25% will die prematurely if unmanaged [19]. Especially in Asian and African countries, and the prevalence of HBV is reported to be as high as 20% of the general population in some countries [20,21]. In most cases, early diagnosis and treatment can prevent HBV from spreading [22]. Currently, two pathways are available for the detection of HBV, including immunoassay and gene analysis. For the former, HBV surface antigen (HBsAg), a typical biomarker of HBV, is usually adopted for the assay using the classic enzyme linked immunosorbent assay (ELISA) for example [23]. However, as is known, there are some limitations of immunoassay, such as false positive results, high cost of monoclonal antibody, and unsatisfactory detection limit. In the case of the gene analysis, real-time quantitative PCR is mostly used [24]. Owing to the highly efficient amplification, real-time quantitative PCR may be more sensitive. Nevertheless, expensive instruments and experienced testers are usually required. Recently, some novel methods have also been developed for the detection of HBV, e.g. smart amplification process (SMAP) [25] and branched chain DNA (bDNA) assay [26]. Each has its advantages and drawbacks. For example, SMAP is time saving but not so convenient; bDNA assay is accurate but not sensitive enough. Therefore, new methods with better performance especially with better cost-effectiveness for the developing countries are still badly required.

In this study, we present a new strategy for colorimetric detection of DNA based on DNA-templated copper nanoclusters. Although some researchers have studied the fluorescence of CuNCs, the analysis of fluorescence signals usually acquired expensive equipment and fluorescence probes. Therefore, fluorescent CuNCs-based assays are difficult to be used widely in developing countries. Here, colorimetric analysis of CuNCs was firstly applied for detection of the DNA. Moreover, our method had some advantages: firstly, colorimetric method could be read out easily with the naked eye, avoiding using equipment. Therefore, our method is extremely attractive for developing countries. Secondly, our method is cost-effective and nontoxic for using copper nanoclusters. Finally, our approach targets HBV, which is an infectious disease in developing countries. The good performance of this assay exhibits its potential application in analysis of DNA related disease, especially in the areas with absence of scientific instruments.

2. Experimental

2.1. Reagents and materials

Copper sulfate ($CuSO_4$), hydrogen peroxide (H_2O_2), hydrochloric acid (HCl), nitric acid (HNO_3) and histidine were bought from Sangon Biotechnology Company (shanghai, china). Ascorbic acid (AA), creatinine, Ethylenediaminetetraacetic acid (EDTA), 2,2′-Azino-bis(3-ethylbenzothiazoline-6-sulfonic acid) diammonium salt (ABTS), Tris (hydroxymethyl) aminomethane (Tris–HCl), sodium chloride (NaCl), 4-morpholinepropanesulfonic acid (MOPS), and sodium acetate (NaAc) were purchased from Sigma–Aldrich (St. Louis, MO, U.S.A.).

Ultrapure water obtained from a Millipore water purification system (≥18 MΩ, Milli-Q, Millipore) was used in all assays.

All purified DNA oligonucleotides were obtained from Sangon Biotechnology Company, and their sequences were listed in Table 1. DNA stock solutions were prepared by dissolving DNA in water and stored at −20 °C.

2.2. Instrumentation

UV–Vis absorption spectra were recorded by an UV-2450 UV/Vis Spectrophotometer (Shimadzu, JPN) from 350 nm to 500 nm [15]. The images of PCR tubes were captured with a Gel Doc XR documentation system (Bio-Rad, USA). A thermostats cultivating shaker (Eppendorf, Germany) was used to provide a certain temperature and rotation speed in the experiment. A thin layer of gold was sputtered by using EMS150 T Sputter Coater (USA-EMS). Atomic force microscope (AFM) 5500 (USA-Agilent Technologies) was used to study the gold layer. Transmission electron microscopy (TEM) measurements were made on a JEOL-2100 transmission electron microscope (JEOL, Japan) and operated at 200 kV.

2.3. Synthesis of DNA-template copper nanoparticles

0.2 μM probe DNA and 0.2 μM target DNA were added into 20 mM MOPS buffer (pH 7.4) [27]. The mixed solution was heated to 90 °C for 10 min and then slowly cooled down to room temperature. After the trial hybridization, the trial was mixed with 100 μM $CuSO_4$ and 1 mM AA, and then the copper nanoparticles were formed with dsDNA templates at 25 °C for 15 min [16]. The formation of CuNPs on the template of dsDNA was examined by TEM. The absorbance of the mixing solution was measured at 420 nm.

Table 1
Sequences of oligonucleotides.

Oligonucleotides	DNA sequences (5′–3′)
Probe DNA	5′-SH-(CH2)6-TCC TGG AAT TAG AGG-3′
Target DNA(T)	5′-ATG TTG CCC GTT TGT CCT CTA ATT CCA GGA-3′
Unmatched variant of T (uT)	5′-GTA GTC GTG ATG AAC GTA TG-3′
3-bases mutation of T (M3)	5′-ATG TTG CCC GTT TGT *ACT GTA TTT* CCA GGA-3′

2.4. DNA detection

As is known, thiol group may attach to the gold surface through an "Au–S" bond. In order to facilitate the immobilization of thiolated DNA probe, a 96-well plate was first sputtered with a thin layer of Au using EMS150 T Sputter Coater. The Au-coated plate was characterized under AFM. As shown in the AFM image of Fig. 1, the gold layer shows a homogeneous and smooth planar sheet appearance, which is favorable for the immobilization of thiolated DNA probe. Thereafter, 12×10^{13} thiolated probe DNA molecules was added into the Au-coated well, and sealed overnight to allow the immobilization. Plate was rinsed with ultrapure water three times, then incubated with 1 mM MCH for 1 h, and rinsed again. Afterward adding 12×10^{13} target DNA molecules (or human serums which were collected from three healthy volunteers and were spiked with different concentrations the target DNA) to form dsDNA template, and incubated for 2 h at 25 °C. Following that, rinsed the plate again. Then a mixture of 1 mM AA and 100 μM $CuSO_4$ were added in 20 mM MOPS buffer solution, then incubated for 10 min at 25 °C. Using Tris–EDTA buffer (10 mM Tris Base, 1 mM EDTA, pH 7.4) rinsed the plate three times, then added 50 mM HNO_3 and incubated 10 min at 25 °C. Transferred the above mixture solution to a PCR tube, and mixed with 200 mM NaAc, 200 μM creatinine, 0.1% H_2O_2 and 2 mM ABTS to produce the color change. Finally, the solution was detected by ultraviolet spectrophotometer.

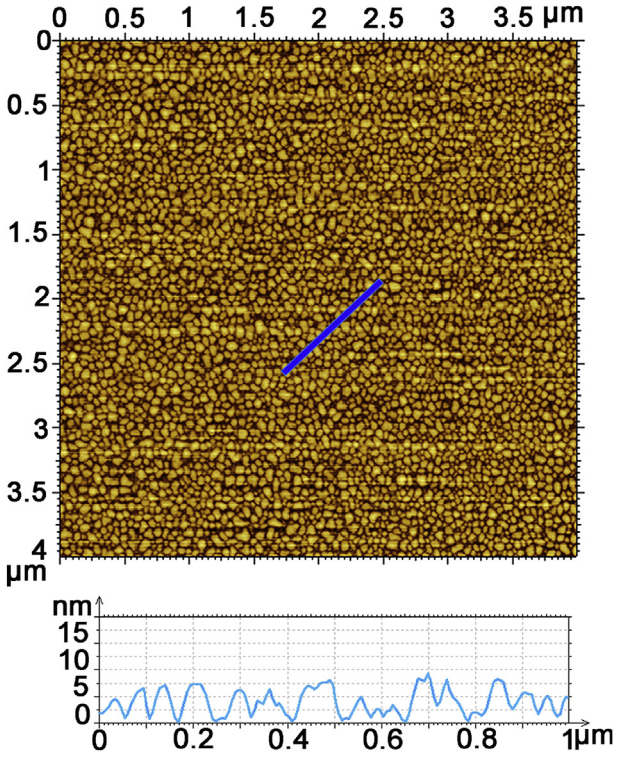

Fig. 1. Atomic force microscopy images of Au layer within the 96-well plate.

3. Results and discussion

3.1. Principle

The schematic illustration of this strategy is represented in Scheme 1. The capture probe is immobilized on the surface of 96-well plate. In the presence of target DNA, target DNA hybridizes the capture probe to form dsDNA. Through the reduction of $CuSO_4$ by AA, dsDNA can be used as efficient templates for the formation of CuNCs [28]. Compared to DNA–AgNCs, CuNCs selectively formed on a DNA duplex, and ensure excellent selectivity [29]. After addition of HNO_3, the CuNCs can be oxidized into copper ions [30]. Adding creatinine to obtain copper–creatinine complex, which appears to possess exceptional metal mimic enzyme properties and rapidly convert H_2O_2 and ABTS into oxidized ABTS [31,32]. The oxidized ABTS was color in green and absorbed at 420 nm [33]. Varying amounts of target DNA would lead to different degree of ABTS oxidation reaction. In this way, our colorimetric detection of DNA is suitable for quantitative and qualitative analysis of DNA. Most importantly, this method has ability to be monitored by the naked eye. Hence, it is an ideal analysis method for instrument-free diagnostic system for detecting genetic disease in developing countries.

3.2. Synthesis and characterization of CuNCs

Firstly, we used HBV DNA as target to examine the feasibility of our method. Since lots of factors e.g. the characterization of CuNCs, catalytic properties and catalytic conditions were important parameters, extensive trials on characterization of CuNCs, chelators for copper ions complex, optimization of catalytic conditions, selectivity, sensitivity of DNA detection, and stability of the colorimetric signals were carried out. The synthesis and characterization of CuNCs were investigated by TEM, UV–Vis spectrophotometer and Gel imaging system, which provided the direct evidence of the formation of CuNCs. The UV–vis absorbance spectra were depicted in Fig. 2A. Fig. 2A shows the UV–vis absorption of the samples as well as the appearance under UV light. The UV–vis results suggest that Cu^0 can form independent of DNA, representing an absorption peak at 340 nm [34]. However, only with dsDNA (probe DNA and target DNA hybridization), the dsDNA-templated CuNCs fluoresce, representing a white color under UV light in black-and-white imaging. That is, the absorption at 340 nm suggests the reduction of Cu^{2+} to Cu^0. And, the fluorescence suggests the presenting of dsDNA and the formation of dsDNA-templated CuNCs. TEM also provides direct evidence of the formation of dsDNA-templated CuNCs. As is shown in Fig. 2B, spherical particles with an average diameter of ca. 6 nm could be clearly observed, suggesting the formation of CuNCs. While without dsDNA template, no similar spherical particles can be observed (data not shown). The TEM result confirms that CuNCs can form on dsDNA template.

3.3. Select chelators for copper ions complex

As is shown in Scheme 1, two key steps are required: 1. the formation of dsDNA-templated CuNCs. 2. the redissolving of CuNCs

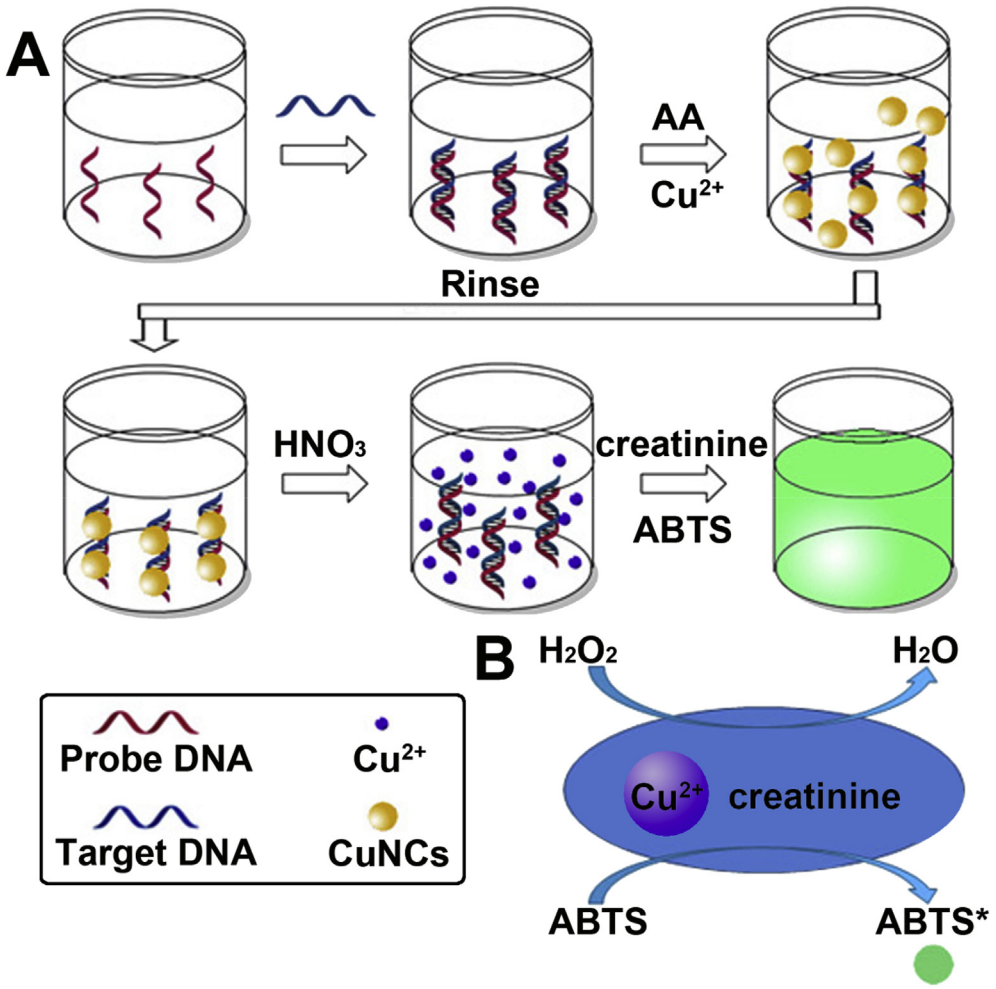

Scheme 1. (A) Schematic illustration of colorimetric detection of DNA based on DNA-templated copper nanoclusters. (B) The principle of DNA detection using a peroxidase-like copper–creatinine complex.

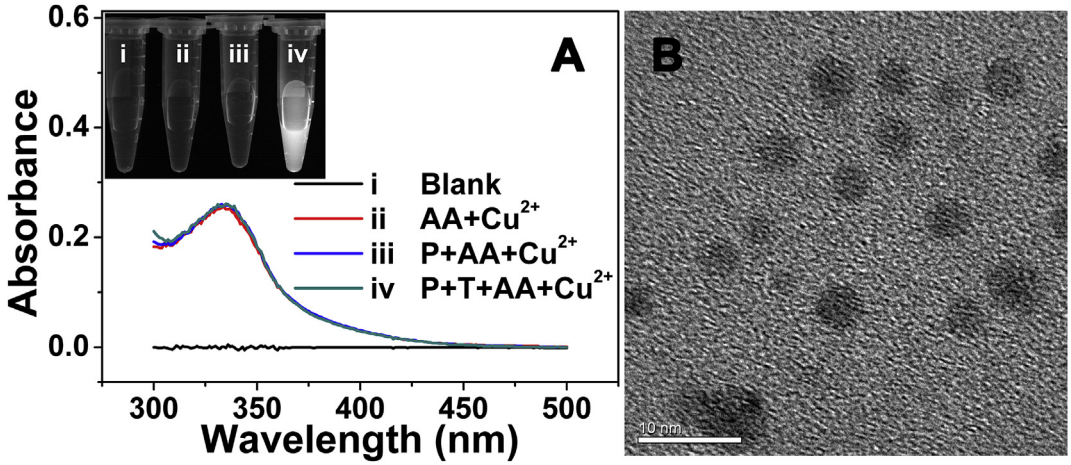

Fig. 2. (A) UV–vis absorbance spectra of different solutions. (i) MOPS buffer only; with addition of (ii) AA and CuSO4; (iii) Probe DNA (P), AA and CuSO4; (iv) Target DNA (T), Probe DNA, AA and CuSO4. Inset: ultraviolet image of above four solutions. All solutions contained 20 mM MOPS buffer solution (pH = 7.4). 2.4×10^{13} Probe DNA molecules, 2.4×10^{13} Target DNA molecules, 100 μM CuSO4 and 1 mM AA were used in the analysis reaction. The mixture incubated for 15 min at 25 °C. Inset: ultraviolet image of four above solution. (B) TEM image of formed CuNPs on dsDNA.

to Cu^{2+} and its catalysis. Since the former one has been addressed in the above section. Here, we study the catalysis of Cu^{2+} and its colorimetric presentation. Different chelators were adopted to enhance the catalytic ability of Cu^{2+}. An ABTS–H_2O_2 reaction

system was also adopted to facilitate a colorimetric observation.

To investigate the effects of different chelators on the catalytic activities of copper ions, the color change of oxidized product (oxidized ABTS) was observed with naked eye. After several preliminary experiments, we selected three chelators (EDTA, creatinine, and histidine) to further optimizing. All experiments were carried out in 50 mM NaAc buffer solution including 2 mM of ABTS, 0.1% H_2O_2, different concentration of copper ions (1 mM, 100 μM, 1 μM, and 10 mM) and chelators (2 mM, 200 μM, 20 μM, and 2 μM). The solution containing no chelator was used as control.

Direct evidence was illustrated in Fig. 3. When EDTA was added, the solution converted to colorless. This result demonstrated that EDTA is a powerful metal chelating agent [35]. That may due to EDTA binds strongly to a wide range of metals [36]. EDTA is known to be used in blood collection. In our strategy, the catalysis step of Cu^{2+} separates from the introduction of the target DNA from clinical samples. So, the EDTA used in blood collection may do no effect to our detection system. In contrast, the group of creatinine displayed obvious color change, including 2 mM creatinine and 1 mM copper ions, 200 μM creatinine and 100 μM copper ions, respectively. The result clearly indicated that the copper ions had high catalytic capability within creatinine. The same result was found in other researches [31,37]. Compare to the control of no chelator, the color of the solution of adding 1 mM copper ions was light green. The result indicated that ABTS could response directly to 1 mM copper ions and produce background signal. Meanwhile, the solution of adding 100 μM copper ions was colorless. Therefore, in order to decrease background signal, we selected 100 μM copper ions in the next step.

In the case of the Cu–histidine complex, the color change was weaker than that observed in the Cu–creatinine complex [38]. What is more, creatinine is more cost-effective than histidine, the Cu–creatinine complex was thus adopted to achieve catalytic oxidation of ABTS to oxidized ABTS. Thus, we selected 100 μM copper ions and 200 μM creatinine in the further experiments.

3.4. Optimization of catalytic conditions

We tested different concentration of strong acids (HNO_3 or HCl), which could convert CuNCs into copper ions [31]. However, ABTS would be oxidized directly by strong acid in the absence of Cu–-creatinine complex. Therefore, in this experiment, we chose NaAc and Tris–HCl in different concentration to adjust the acidity of the solution. First, the different concentration of NaAc and Tris–HCl were added in different columns of 96-well plate, respectively. In addition, different concentration of HNO_3 and HCl were added in different lines of 96-well plate, respectively. Then, the solution followed by addition of 100 μM $CuSO_4$ or not to incubate with 200 μM creatinine, 0.1% H_2O_2, and 2 mM ABTS for 10 min at room temperature. In this process, the color changes of ABTS–H_2O_2 reaction could be observed within 10 min by naked eye.

The results as depicted in Fig. 4. The addition of Tris–HCl and HNO_3, no obvious color change was observed. The result revealed that the simultaneous addition of Tris–HCl and HNO_3 has little influence on the catalytic activity, which may be owing to Tris-base. Tris-base could catalyze the reaction of copper ions to produce copper hydroxide, which sharply reduced the reaction between copper ions and creatinine [39]. However, in the group of HCl, significant color change was observed without addition of copper ions. The phenomenon revealed that ABTS-H_2O_2 complexes direct responded to HCl. HCl resulted obvious background signal therefore it is not suitable catalytic condition.

As shown in red (in the web version) box of Fig. 4, under the condition of 50 mM HNO_3 and 200 mM NaAc, the color change in the presence of $CuSO_4$ was distinct. Meanwhile, the control group without $CuSO_4$ showed inconspicuous change. According to these results, 200 mM NaAc and 50 mM HNO_3 were chosen as the optimum catalytic conditions for the colorimetric assay.

3.5. Selectivity of DNA detection

During the gene analysis for therapy purpose, detection of single nucleotide polymorphisms (SNPs) is also important [40]. Here, we

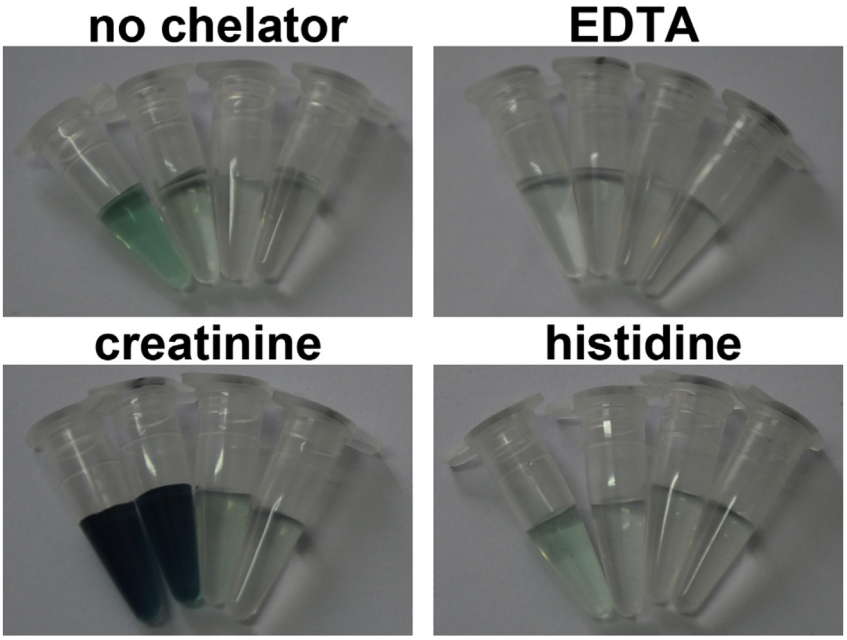

Fig. 3. Select chelators for copper ions complex. These chelators were EDTA, creatinine and histidine. The group of no chelator was control. All experiments were carried out in 50 mM NaAc buffer solution including 2 mM ABTS, 0.1% H_2O_2 and different concentration of copper ions and chelators (from left to right: 1 mM copper ions and 2 mM chelators; 100 μM copper ions and 200 μM chelators, 10 μM copper ions and 20 μM chelators, 1 μM copper ions and 2 μM chelators). All solution mixed entirely and incubated for 15 min at 25 °C.

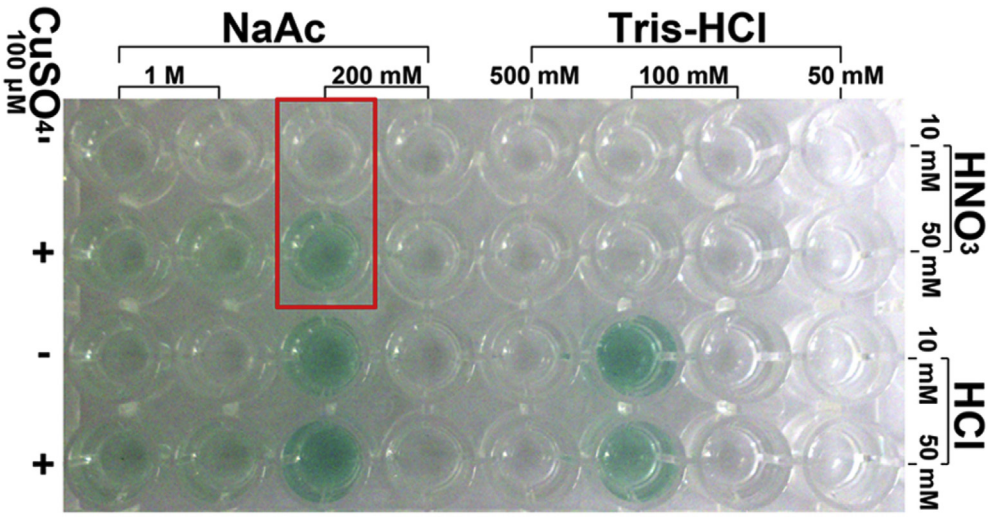

Fig. 4. Optimization of catalytic conditions. The different concentration of NaAc (200 mM and 1 M) or Tris–HCl (50 mM, 100 mM, and 500 mM) were chosen to determine the optimal condition. In addition, different concentration of HNO_3 (10 mM and 50 mM) and HCl (10 mM and 50 mM) was added into the mixtures. Then, the solution followed by addition of 100 μM $CuSO_4$ (+) or not (−) to incubate with 200 μM creatinine, 0.1% H_2O_2, and 2 mM ABTS for 10 min at 25 °C.

further investigated the sequence selectivity of this method with naked eye and examined the ultraviolet absorptions of the probe DNA (P) toward three-base mismatched target DNA (M3), un-complementary target DNA (uT), and target DNA (T). The amount of probe DNA, target DNA, M3 and uT were 12×10^{13} molecules, respectively. As shown the insert in Fig. 5A, only the sample containing probe DNA and complementary target DNA (P + T) exhibited extremely sharp color transitions, which have been used to enhance the selectivity of detection systems. It is easy to identify the addition of target DNA by naked-eye. The same result was obtained from UV–vis absorbance spectra. Only adding target probe, a high absorption peak at 420 nm can be detected. All the absorption peaks for 3-bases mutants and un-complementary sequence were much lower than that for the target DNA. The absorbance percentage of P + M3 and P + uT comparing to P + T were 10.48% and 10.90%, respectively (Fig. 5B). These results further confirmed that this method was sensitive enough to distinguish between three base differences.

3.6. Sensitivity of DNA detection

Under the optimization condition, we evaluated the capability of our method for quantitative detection of target DNA. The concentration of target DNA was covered a range of nearly 6 orders of magnitude (from 0 to 12×10^{13} molecules). As shown in Fig. 6A, the UV–vis absorbance increased with increment of target DNA concentration in the sample. However, it did not change significantly when the concentration of the target DNA was increased from 0 min to 12×10^{8} molecules. As the concentration of target increased up to 12×10^{9} molecules, a gradual increase in the spectrum intensity was observed. The same result was observed in the image of samples (Fig. 6A, insert). Adding 12×10^{9} molecules target probe produced easily visible differences. The result demonstrated that the addition of 12×10^{9} target DNA molecules gave rise to an obvious increase in the catalytic activity. With the increase of target DNA, the color changes of the solution become more obvious. These results indicated that more oxidized ABTS were formed in the mixture when more target probes were added, as expected. These results revealed our method for DNA detection is effective.

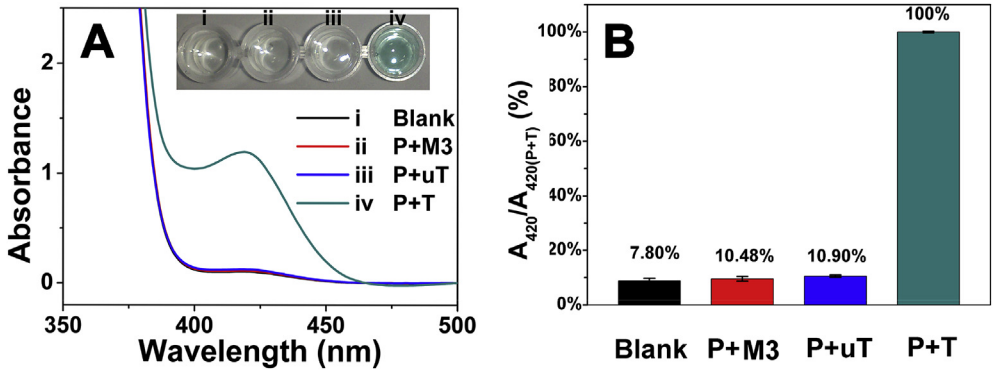

Fig. 5. (A) UV–vis absorbance spectra of selective polynucleotide detection for the target probes. All solution contained 200 mM NaAc and 50 mM HNO_3 buffer solution, 100 μM $CuSO_4$, 1 mM AA, 200 μM creatinine, 0.1% H_2O_2, 2 mM ABTS and incubated at 25 °C under different DNA hybridize conditions: (i) without DNA (ii) 12×10^{13} Probe DNA molecules and 12×10^{13} M3 molecules (three-base mismatched target DNA) (iii) 12×10^{13} Probe DNA molecules and 12×10^{13} uT molecules (un-complementary Target DNA) (iv) 12×10^{13} Probe DNA molecules and 12×10^{13} Target DNA molecules. Inset: the picture of four above solution. (B) Absorbance percentage of P + M3 and P + uT comparing to P + T; error bar ± S.D. (n = 3).

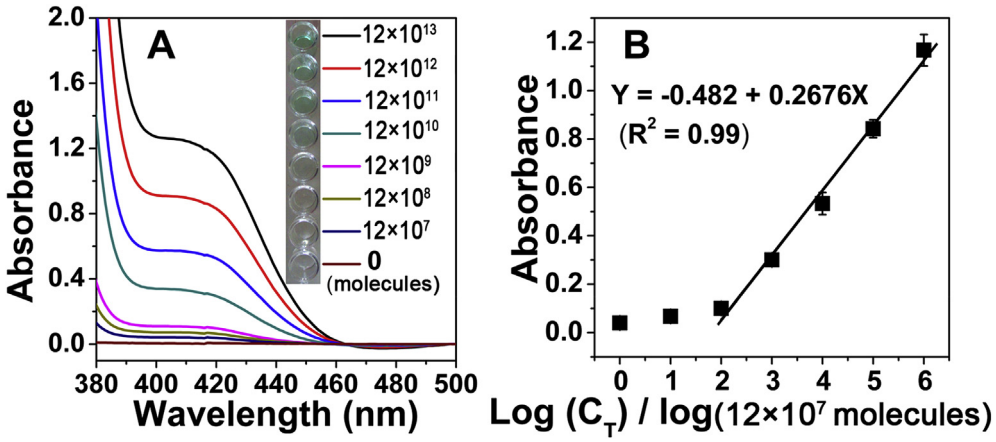

Fig. 6. (A) UV–vis absorbance spectra of the solution with different concentrations of target DNA (up to down: 12×10^{13}, 12×10^{12}, 12×10^{11}, 12×10^{10}, 12×10^{9}, 12×10^{8}, 12×10^{7} and none molecules). Inset: the picture of above solutions. (B) The linear relationship between the ultraviolet absorbance and logarithm of concentration of target DNA. Other conditions are the same as that in Fig. 5A.

Fig. 6B outlined the relationship between the UV–vis absorbance at 420 nm (the maximal absorption of oxidized ABTS) and logarithm (log) of concentration of target DNA in the range from 0 to 12×10^{13} molecules. Calibrated colorimetric measurements could be used to determine the amount of target quantitatively. The linear curve fitted a regression equation of $Y = -0.482 + 0.2676X$. The correlation coefficient of $R^2 = 0.99$ within a range from 12×10^9 molecules to 12×10^{13} molecules. From Fig. 6B, it was found that the addition of 12×10^9 target DNA molecules gave rise to an obvious increase in the catalytic activity, indicating a detection limit of 12×10^9 molecules for analyzing DNA. The sensitivity of our method is not so satisfactory to monitor early infection of HBV on therapy. However, considering that some currently available methods with considerable sensitivity, e.g. COBAS® system from Roche Inc., are costly and not suitable for low-resource areas, our method may serve a suitable, rapid and not costly DNA-quantitative test for these country.

3.7. Stability of the colorimetric signals

The stability of the colorimetric signals is of great importance for delayed measurements. Here, the colorimetric signals for the detection of 12×10^{13} molecules of the HBV DNA were used for the stability assay. The absorbance was determined at 420 nm at 10 min, 30 min, 1 h, 6 h, 1 day, 3 days, and 7 days after reactions. The absorbance at each time point was corrected for the absorbance of an ABTS blank. As shown in Fig. 7, the absorbance at 420 nm decreased slowly along time. Nevertheless, the absorbance remained 95% of its original intensity after 7 days, indicating a favorable stability.

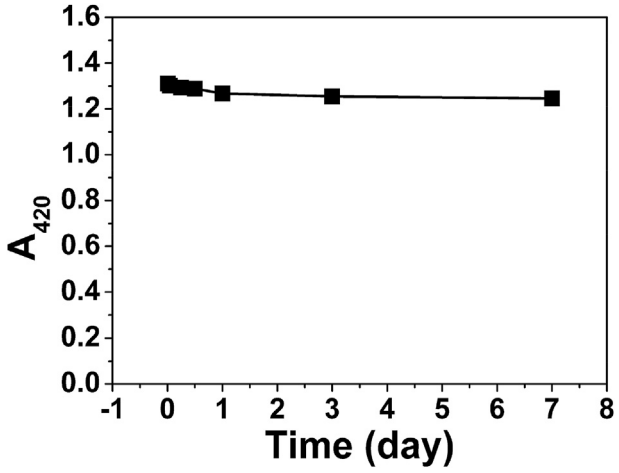

Fig. 7. The stability of the absorbance for the detection of 12×10^{13} molecules of the HBV DNA.

Table 2
Detection of HBV positive serums. The serums were collected from three healthy volunteers. Different concentrations of HBV DNA were spiked. Each serum sample was tested for three times ($n = 3 \times 3 = 9$).

Sample number	Added (nM)	Found (nM)	Recovery (%)	RSD (%) (n = 9)
1	1	1.31	131%	7.2
2	10	11.5	115%	4.9
3	100	90.4	90.4%	6.0

3.8. Detection of HBV positive serum

Human serums were separated from blood of healthy volunteers, different concentrations of HBV DNA were spiked into serum samples and were tested for our analysis method. As shown in Table 2, the results showed that acceptable recoveries and relative standard deviation (RSD) could be obtained, indicating the potential application of our methodology for clinical applications.

4. Conclusion

In summary, we have developed a colorimetric detection method of ssDNA based on DNA-templated copper nanoclusters. In comparison with other DNA analysis techniques, our approach provides several advantages that will meet demands of poverty areas. The attributes of this detection as follows: first of all, the products could be visualized by naked-eye without requiring advanced laboratory equipment. Secondly, CuCNs own the characteristic of low-cost and unique physicochemical properties that can be easily applied, making them ideal candidates for biochemical analysis. The assay we have described has additional benefits beyond cost-efficiency. Furthermore, this method can be utilized to identify three base-pair mismatches displaying potential application for the detection of important genetic basis of disease. Finally, this strategy can detect target DNA with a detection limit of 12×10^9 molecules. Inspired by these advantageous features, we

conclude that our method is a highly attractive candidate in DNA analysis, especially early diagnosis of genetic diseases in developing countries without complicated equipment and expensive solvents.

Acknowledgment

This work is supported by the National Natural Science Foundation of China (Grant No. 31200742).

References

[1] H.X. Li, L.J. Rothberg, Label-free colorimetric detection of specific sequences in genomic DNA amplified by the polymerase chain reaction, J. Am. Chem. Soc. 126 (2004) 10958–10961.
[2] Z. Taleat, K. Mathwig, E.J. Sudhölter, L. Rassaei, Detection strategies for methylated and hypermethylated DNA, TrAC Trends Anal. Chem. 66 (2015) 80–89.
[3] C.A. Chen, C.C. Wang, Y.J. Jong, S.M. Wu, Label-free fluorescent copper nanoclusters for genotyping of deletion and duplication of Duchenne muscular dystrophy, Anal. Chem. 87 (2015) 6228–6232.
[4] Y. Xiao, A.A. Lubin, B.R. Baker, K.W. Plaxco, A.J. Heeger, Single-step electronic detection of femtomolar DNA by target-induced strand displacement in an electrode-bound duplex, Proc. Natl. Acad. Sci. U. S. A. 103 (2006) 16677–16680.
[5] J.M. Hu, Y.J. Yu, J.C. Brooks, L.A. Godwin, S. Somasundaram, F. Torabinejad, J. Kim, C. Shannon, C.J. Easley, A reusable electrochemical proximity assay for highly selective, real-time protein quantitation in biological matrices, J. Am. Chem. Soc. 136 (2014) 8467–8474.
[6] J.M. Hu, T.Y. Wang, J. Kim, C. Shannon, C.J. Easley, Quantitation of femtomolar protein levels via direct readout with the electrochemical proximity assay, J. Am. Chem. Soc. 134 (2014) 7066–7072.
[7] J.S. Lee, M.S. Han, C.A. Mirkin, Colorimetric detection of mercuric ion (Hg2+) in aqueous media using DNA-functionalized gold nanoparticles, Angew. Chem. Int. Ed. 119 (2007) 4171–4174.
[8] L.B. Zhang, E. Wang, Metal nanoclusters: new fluorescent probes for sensors and bioimaging, Nano Today 9 (2014) 132–157.
[9] J.G. Li, T.T. Zhao, T.K. Chen, Y. Liu, C.N. Ong, J. Xie, Engineering noble metal nanomaterials for environmental applications, Nanoscale 7 (2015) 7502–7519.
[10] S. Clède, C. Policar, Metal-carbonyl units for vibrational and luminescence imaging: towards multimodality, Chem. Eur. J. 21 (2015) 942–958.
[11] S. Chattoraj, K. Bhattacharyya, Fluorescent gold nanocluster inside a live breast cell: etching and higher uptake in cancer cell, J. Phys. Chem. C 118 (2014) 22339–22346.
[12] S.M. Copp, D.E. Schultz, S. Swasey, E.G. Gwinn, Atomically precise arrays of fluorescent silver clusters: a modular approach for metal cluster photonics on DNA nanostructures, ACS Nano 9 (2015) 2303–2310.
[13] X. Tian, X.J. Kong, Z.M. Zhu, T.T. Chen, X. Chu, A new label-free and turn-on strategy for endonuclease detection using a DNA-silver nanocluster probe, Talanta 131 (2015) 116–120.
[14] L. Dong, J.B. Zang, L. Su, Y.D. Jia, Y.H. Wang, J. Lu, X.P. Xu, Oxidized carbon/nano-SiC supported platinum nanoparticles as highly stable electrocatalyst for oxygen reduction reaction, Int. J. Hydrogen Energy 39 (2014) 16310–16317.
[15] Z.X. Zhou, Y. Du, S.J. Dong, Double-strand DNA-templated formation of copper nanoparticles as fluorescent probe for label-free aptamer sensor, Anal. Chem. 83 (2011) 5122–5127.
[16] N. He, S.N. Xu, Molecular-dynamics simulation of structure change for a molten Cu 297 nanocluster during rapidly quenching, Adv. Mater. Res. 652–654 (2013) 267–271.
[17] Y.C. Guo, S.C. Sheng, B. Nie, Z.G. Tu, Development of magnetic capture hybridization and quantitative polymerase chain reaction for hepatitis B virus covalently closed circular DNA, Hepat. Mon. 15 (2015) e23729.
[18] H. Thorsteinsdóttir, U. Quach, A.S. Daar, P.A. Singer, Conclusions: promoting biotechnology innovation in developing countries, Nat. Biotechnol. 22 (2004) DC48–DC52.
[19] J.J. Otta, G.A. Stevensa, J. Groegerb, S.T. Wiersmaa, Global epidemiology of hepatitis B virus infection: new estimates of age-specific HBsAg seroprevalence and endemicity, Vaccine 30 (2012) 2212–2219.
[20] E.W. Hwang, R. Cheung, Global epidemiology of hepatitis B virus (HBV) infection, N A J. Med. Sci. 4 (2011) 7–13.
[21] C.J. Chen, L.Y. Wang, M.W. Yu, Epidemiology of hepatitis B virus infection in the Asia-Pacific region, J. Gastroenterol. Hepatol. 15 (2000) E3–E6.
[22] J. Bruix, A.J. Hessheimer, A. Forner, L. Boix, R. Vilana, J.M. Llovet, New aspects of diagnosis and therapy of hepatocellular carcinoma, Oncogene 25 (2006) 3848–3856.
[23] Q.Y. He, G.K.K. Lau, Y. Zhou, S.T. Yuen, M.C. Lin, H.F. Kung, J.F. Chiu, Serum biomarkers of hepatitis B virus infected liver inflammation: a proteomic study, Proteomics 3 (2003) 666–674.
[24] D. Candotti, J. Temple, S.O. Ofori, J.P. Allain, Multiplex real-time quantitative RT-PCR assay for hepatitis B virus, hepatitis C virus, and human immunodeficiency virus type 1, J. Virol. Methods 118 (2004) 39–47.
[25] J. Yang, J. Li, G.Q. Lou, L.J. Wu, C. Feng, N.P. Wu, Rapid identification of YVDD mutants of hepatitis B virus using smart amplification process with competition probe, Acta Virol. 55 (2011) 295–302.
[26] K.R. Loeb, K.R. Jerome, J. Goddard, M. Huang, A. Cent, L. Corey, High-throughput quantitative analysis of hepatitis B virus DNA in serum using the TaqMan fluorogenic detection system, Hepatology 32 (2000) 626–629.
[27] F. Sousa, G.M. Guebitz, V. Kokol, Antimicrobial and antioxidant properties of chitosan enzymatically functionalized with flavonoids, Process Biochem. 44 (2009) 749–756.
[28] J.H. Chen, J. Liu, Z.Y. Fang, L.W. Zeng, Random dsDNA-templated formation of copper nanoparticles as novel fluorescence probes for label-free lead ions detection, Chem. Commun. 48 (2012) 1057–1059.
[29] X.M. Yang, Y. Zhuo, S.S. Zhu, Y.W. Luo, Y.J. Feng, Y. Xu, Selectively assaying CEA based on a creative strategy of gold nanoparticles enhancing silver nanoclusters' fluorescence, Biosens. Bioelectron. 64 (2015) 345–351.
[30] S. Paul, R. Clérac, N.G. Hearns, D. Ray, Novel layering of aqua and imidazolidinyl phenolate bridged cationic $[Cu^{II}_2(\mu\text{-}L)(\mu\text{-}H_2O)\cdot H_2O]_2$ units over $Cu^{I}NCS$ based one-dimensional anionic parallel chains as diamagnetic coordination framework host, Cryst. Growth Des. 9 (2009) 4032–4040.
[31] A. Singh, S. Patra, J.A. Lee, K.H. Park, H. Yang, An artificial enzyme-based assay: DNA detection using a peroxidase-like copper-creatinine complex, Biosens. Bioelectron. 26 (2011) 4798–4803.
[32] M.J. Pugia, J.A. Lott, J.F. Wallace, T.K. Cast, L.D. Bierbaum, Assay of creatinine using the peroxidase activity of copper-creatinine complexes, Clin. Biochem. 33 (2000) 63–70.
[33] M. Solís-Oba, V.M. Ugalde-Saldívar, I. González, G. Viniegra-González, An electrochemical-spectrophotometrical study of the oxidized forms of the mediator 2, 2′-azino-bis-(3-ethylbenzothiazoline-6-sulfonic acid) produced by immobilized laccase, J. Electroanal. Chem. 579 (2005) 59–66.
[34] X.P. Wang, B.C. Yin, B.C. Ye, A novel fluorescence probe of dsDNA-templated copper nanoclusters for quantitative detection of microRNAs, RSC Adv. 3 (2013) 8633–8636.
[35] R. Kunkel, S.E. Manahan, Atomic absorption analysis of strong heavy metal chelating agents in water and waste water, Anal. Chem. 45 (1973) 1465–1468.
[36] P.S. Rendell, G.E. Batley, A.J. Cameron, Adsorption as a control of metal concentrations in sediment extracts, Environ. Sci. Technol. 14 (1980) 314–318.
[37] G. Multhaup, T. Ruppert, A. Schlicksupp, L. Hesse, E. Bill, R. Pipkorn, C.L. Masters, K. Beyreuther, Copper-binding amyloid precursor protein undergoes a site-specific fragmentation in the reduction of hydrogen peroxide, Biochemistry 37 (1998) 7224–7230.
[38] H. Kodama, C. Fujisawa, W. Bhadhprasit, Inherited copper transport disorders: biochemical mechanisms, diagnosis, and treatment, Curr. Drug Metab. 13 (2012) 237–250.
[39] G. Allen, Specific protein degradation by copper (II) ions, Met. Ions Biol. Syst. 38 (2001) 197–212.
[40] P.K. Gupta, J.K. Roy, M. Prasad, Single nucleotide polymorphisms (SNPs): a new paradigm in molecular marker technology and DNA polymorphism detection with emphasis on their use in plants, Curr. Sci. 80 (2001) 524–535.